Singlet Oxygen Is the Major Reactive Oxygen Species Involved in Photooxidative Damage to Plants[1][W]

Christian Triantaphylidès*, Markus Krischke, Frank Alfons Hoeberichts, Brigitte Ksas, Gabriele Gresser, Michel Havaux, Frank Van Breusegem, and Martin Johannes Mueller

Commissariat à l'Energie Atomique, Direction des Sciences du Vivant, Institut de Biologie Environnementale et Biotechnologie, Laboratoire de Ecophysiologie Moléculaire des Plantes, and Centre National de la Recherche Scientifique, Unité Mixte de Recherche, Biologie Végétale et Microbiologie Environnementale, and Université d'Aix Marseille, F–13108 Saint Paul lez Durance, France (C.T., B.K., M.H.); Pharmaceutical Biology, Julius-von-Sachs-Institute for Biosciences, University of Wuerzburg, D–97082 Wuerzburg, Germany (M.K., G.G., M.J.M.); and Department of Plant Systems Biology, Flanders Institute for Biotechnology, and Department of Molecular Genetics, Ghent University, 9052 Ghent, Belgium (F.A.H., F.V.B.)

Reactive oxygen species act as signaling molecules but can also directly provoke cellular damage by rapidly oxidizing cellular components, including lipids. We developed a high-performance liquid chromatography-electrospray ionization-tandem mass spectrometry-based quantitative method that allowed us to discriminate between free radical (type I)- and singlet oxygen ($^1O_2$; type II)-mediated lipid peroxidation (LPO) signatures by using hydroxy fatty acids as specific reporters. Using this method, we observed that in nonphotosynthesizing Arabidopsis (*Arabidopsis thaliana*) tissues, nonenzymatic LPO was almost exclusively catalyzed by free radicals both under normal and oxidative stress conditions. However, in leaf tissues under optimal growth conditions, $^1O_2$ was responsible for more than 80% of the nonenzymatic LPO. In Arabidopsis mutants favoring $^1O_2$ production, photooxidative stress led to a dramatic increase of $^1O_2$ (type II) LPO that preceded cell death. Furthermore, under all conditions and in mutants that favor the production of superoxide and hydrogen peroxide (two sources for type I LPO reactions), plant cell death was nevertheless always preceded by an increase in $^1O_2$-dependent (type II) LPO. Thus, besides triggering a genetic cell death program, as demonstrated previously with the Arabidopsis *fluorescent* mutant, $^1O_2$ plays a major destructive role during the execution of reactive oxygen species-induced cell death in leaf tissues.

Plant leaves capture sun-derived light energy to drive CO_2 fixation during photosynthesis. During this process, leaves need to cope with photooxidative stress when the balance between energy absorption and consumption is disturbed. Excess excitation energy in the photosystems (PSI and PSII) leads to the inhibition of photosynthesis via the production of various reactive oxygen species (ROS) at different spatial levels of the cell (Apel and Hirt, 2004; Asada, 2006; Van Breusegem and Dat, 2006). Both exposure to high light intensities and decreased CO_2 availability direct linear electron transfer toward the reduction of molecular oxygen, generating superoxide radicals ($O_2^{-\cdot}$) at PSI (the Mehler reaction). Superoxide dismutation generates hydrogen peroxide (H_2O_2), which is detoxified in the chloroplast by ascorbate peroxidases. As such, this so-called water-water cycle participates in the dissipation of excess energy (Asada, 2006). Decreased CO_2 availability affects the first step in CO_2 fixation by shifting the carboxylation of Rubisco by the Rubisco carboxylase-oxygenase enzyme toward oxygenation, a process called photorespiration. This leads, through the action of glycolate oxidase, to peroxisomal H_2O_2 production that is counteracted by catalases. Finally, when the intersystem electron carriers are overreduced, triplet excited P680 in the PSII reaction center as well as triplet chlorophylls in the light-harvesting antennae are produced, with the production of singlet oxygen ($^1O_2$) as a consequence (Krieger-Liszkay, 2005). In photosynthetic membranes, $^1O_2$ is quenched by carotenoids and tocopherols. When antioxidant mechanisms are overwhelmed, increased cellular ROS levels trigger signal transduction events related to stress signaling and programmed cell death (Mittler et al., 2004; Van Breusegem and Dat, 2006). On the other hand, excessive ROS accumulation damages pigments, proteins, nucleic acids, and lipids

[1] This work was supported by grants from the exchange programs Tournesol (grant nos. F/11498QB and B/T2006.14) and Procope (grant nos. F/14925QF and D/0628204), in part by the Sonderforschungsbereiche number 567 of the Deutsche Forschungsgemeinschaft (to M.J.M.), and by the Ghent University (Geconcerteerde Onderzoeksacties no. 12051403) and the Research Foundation-Flanders (grant no. G.0350.04).

* Corresponding author; e-mail ctriantaphylid@cea.fr.

The author responsible for distribution of materials integral to the findings presented in this article in accordance with the policy described in the Instructions for Authors (www.plantphysiol.org) is: Christian Triantaphylidès (ctriantaphylid@cea.fr).

[W] The online version of this article contains Web-only data.

www.plantphysiol.org/cgi/doi/10.1104/pp.108.125690

(Halliwell and Gutteridge, 2007), thereby contributing to or executing cell death.

Since under environmental stress conditions different ROS are produced simultaneously, a causal link between the accumulation of a specific ROS and its signaling or damaging effects has always been difficult to establish. In recent years, the production of various transgenic Arabidopsis (*Arabidopsis thaliana*) plants with compromised levels of specific antioxidant enzymes and the identification of the conditional *fluorescent* (*flu*) mutant provided important tools to assess the specific effects of $O_2^{-\cdot}$, H_2O_2, and $^1O_2$ within a particular subcellular compartment (Dat et al., 2003; op den Camp et al., 2003; Pnueli et al., 2003; Rizhsky et al. 2003; Vandenabeele et al., 2004; Wagner et al., 2004; Queval et al., 2007). For example, with catalase-deficient [Cat(−)] plants, the signaling effects of increased photorespiratory H_2O_2 levels could be identified (Dat et al., 2003; Vandenabeele et al., 2004; Queval et al., 2007). Similarly, in the conditional *flu* mutant increased plastid $^1O_2$ levels were shown to induce a genetic program leading to cell death (op den Camp et al., 2003; Wagner et al., 2004). Nevertheless, whereas careful monitoring of gene expression on the whole-genome level enables to pinpoint specific signaling capacities for diverse ROS (Mittler et al., 2004; Gadjev et al., 2006), it remained impossible to discriminate between the oxidative damaging effects on cellular components of different ROS.

One consequence of ROS formation is lipid peroxidation (LPO; Halliwell and Gutteridge, 2007). Two nonenzymatic reaction types lead to specific patterns of oxidized membrane polyunsaturated fatty acids (PUFAs; Stratton and Liebler, 1997; Montillet et al., 2004; Mueller et al., 2006). Type I reactions are initiated by free radicals (FRs) having high redox potential, such as hydroxyl radicals ($^{\cdot}OH$) or organic oxyl and peroxyl radicals, and type II reactions are the result of $^1O_2$ action. Notably, $O_2^{-\cdot}$ and H_2O_2 are not sufficiently reactive to oxidize any PUFA. However, both ROS can be nonenzymatically converted to $^{\cdot}OH$ through Fenton-type reactions in the presence of transition metal ions such as Fe^{2+} (Halliwell and Gutteridge, 2007). Both type I and type II reactions lead to the formation of respective oxygenated fatty acids. Here, we propose a novel and quantitative approach to distinguish between FR- and $^1O_2$-mediated LPO in plants by quantifying type II oxidation-specific hydroxy fatty acids with HPLC-tandem mass spectrometry (MS/MS), allowing us to monitor the relative contribution of LPO caused by PSI-dependent $O_2^{-\cdot}/H_2O_2$, photorespiratory H_2O_2, and photosynthetic $^1O_2$ during photooxidative stress and cell death. We demonstrate that nonenzymatic LPO in leaves is almost exclusively mediated by $^1O_2$ and that photooxidative stress-dependent cell death involves $^1O_2$ production in its final stage.

RESULTS

An LPO Signature That Discriminates between $^1O_2$ and FR-Dependent LPO in Plant Tissues

$^1O_2$ and FRs (as defined above) readily oxidize free and esterified PUFAs with a rate constant almost only limited by diffusion (Elstner, 1982). In both cases, the products are hydroperoxy PUFAs that are reduced in vivo to stable hydroxy fatty acids. We first assessed the differential oxidation of both linoleic (18:2) and linolenic acid (18:3) in vitro. $^1O_2$ production was triggered by O_2 photoactivation with methylene blue (Stratton and Liebler, 1997), whereas FR-mediated oxidation was initiated by H_2O_2 or *tert*-butyl hydroperoxide (BOOH) in the presence of Fe^{2+} (Halliwell and Gutteridge, 2007). After reduction of hydroperoxy PUFAs, hydroxy fatty acids were analyzed by HPLC-negative electrospray ionization-MS/MS. In contrast to gas chromatography-MS based methods (Mueller et al., 2006; Przybyla et al., 2008), HPLC-electrospray ionization-MS/MS does not require derivatization of hydroxy fatty acids and hence allows the direct and quantitative evaluation of all hydroxy fatty acid isomers. $^1O_2$- and FR-mediated peroxidation of both 18:2 and 18:3 can be discriminated and quantified by the hydroxy fatty acid isomer distribution (Supplemental Fig. S1). Since it is the most abundant PUFA in leaves, we opted to analyze further only the 18:3 oxidation products (Fig. 1). Two out of the six possible hydroxy fatty acid isomers, 10-hydroxy-8,12,15(*E*,*Z*,*Z*)octadecatrienoic acid (HOTE) and 15-HOTE, were specific products exclusively formed by $^1O_2$, whereas 9-HOTE, 12-HOTE, 13-HOTE, and 16-HOTE could be both generated through $^1O_2$ or FR catalysis. The comparison of the relative abundance of 10-HOTE and 15-HOTE to that of 9-HOTE and 16-HOTE allowed for a clear distinction between $^1O_2$ and

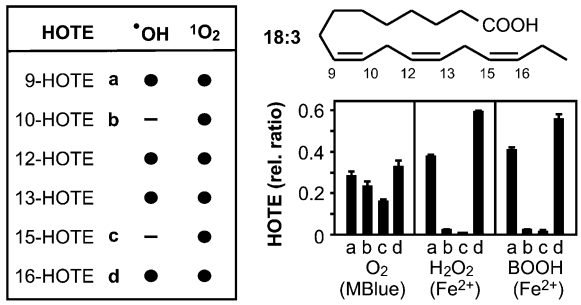

Figure 1. Peroxidation of linolenic acid (18:3). Peroxidation of 18:3 yields 9-, 10-, 12-, 13-, 15-, and 16-(hydro-)peroxy fatty acids, which can be reduced in vitro and in vivo to the corresponding HOTEs. All six theoretical possible isomers are formed by $^1O_2$-mediated oxidation, while FRs such as $^{\cdot}OH$ catalyze only the formation of four isomers. The HOTE signature, described as relative normalized levels of 9-HOTE (a), 10-HOTE (b), 15-HOTE (c), and 16-HOTE (d), characterizes: $^1O_2$-mediated LPO, $^1O_2$ generated by light activation of O_2 in the presence of methylene blue (MBlue); FR-mediated LPO, FR generated from H_2O_2 or *tert*-BOOH through Fe^{2+} catalysis; see "Materials and Methods." Results are expressed as mean ± SD (n = 3).

FR-mediated 18:3 oxidation (Fig. 1). We estimated that it was possible to evaluate a combination of both LPO processes in the proportion between 80%/20% and 20%/80%.

Next, we assessed both LPO processes in planta. Typically, lipid extracts from Arabidopsis tissues were reduced and hydrolyzed before total (free and esterified) hydroxy fatty acids were analyzed. We evaluated ROS-mediated LPO and lipoxygenase (LOX)-dependent LPO by HPLC-UV as previously described (Montillet et al., 2004), and then the $^1O_2$- and FR-mediated LPO using the method established above. To obtain unambiguous observations for FR-mediated LPO, we investigated LPO processes in Arabidopsis cell suspensions and roots. Both tissues are devoid of $^1O_2$-producing photosystems and displayed low basal levels of ROS-mediated LPO (approximately 1–2 nmol g^{-1} fresh weight [FW]) with an almost exclusively FR-mediated HOTE signature (Fig. 2A). Four hours after the addition of BOOH to cell suspensions and H_2O_2 or BOOH to roots, ROS-mediated LPO increased and the HOTE signature was indicative of FR-mediated LPO. Next, we compared HOTE isomer distribution in leaves from Arabidopsis wild-type and *vte1 npq1* plants. The *vte1 npq1* double mutant is sensitive to photooxidative stress due to a deficiency in two lipophilic $^1O_2$ quenchers in the chloroplasts, α-tocopherol and the carotenoid zeaxanthin (Havaux et al., 2005). In both wild-type and *vte1 npq1* leaves, basal levels of HOTE (approximately 5–10 nmol/g FW; Fig. 2, B and C) were approximately 5-fold higher than in roots. The HOTE signature in both wild-type and *vte1 npq1* leaves displayed an almost exclusively $^1O_2$-mediated LPO (Fig. 2, B and C). We then infiltrated the leaves of both plants with a mixture of BOOH and Fe^{3+} to favor the Fenton reaction. After 4 h incubation in the dark, the HOTE signature indicated a shift from a $^1O_2$ LPO mechanism (Fig. 2, B and C, controls) to a mixed $^1O_2$/FR LPO mechanism in treated samples (Fig. 2, B [50% FR-dependent LPO] and C [70% FR-dependent LPO]). Exposure of wild-type plants to photooxidative stress conditions (7°C and 1,300 μmol m^{-2} s^{-1} light) for 26 h at normal CO_2 (380 ppm) and at high CO_2 (2,000 ppm, to inhibit photorespiratory production of H_2O_2) did not increase $^1O_2$-mediated LPO (Fig. 2D) and did not provoke tissue damage (Fig. 2E). However, in *vte1 npq1* a strong $^1O_2$-mediated LPO and tissue damage were observed (Fig. 2, D and F). Notably, total HOTE levels and the isomer distribution patterns were similar under normal and high CO_2 conditions, suggesting that similar levels of $^1O_2$ were produced in the presence or absence of photorespiration. Thus, in *vte1 npq1*, LPO and cell death are strictly correlated with $^1O_2$ production. By comparison, in wild-type plants we observed both delayed $^1O_2$-mediated LPO increase and light-induced damage that became only apparent after 54 h (data not shown).

Taken together, these results demonstrate that the HOTE signature determined by HPLC-electrospray ionization-MS/MS allows us to discriminate between FR- and $^1O_2$-mediated LPO processes in plant tissues.

$^1O_2$ Generation Induces Cell Death in Arabidopsis Leaf Tissues

In leaves of the *flu* mutant, a genetic cell death program can be triggered by protochlorophyllide-dependent $^1O_2$, involving 13-LOX LPO, and apparently occurs without any increase of nonenzymatic LPO early in the signaling phase, whereas in etiolated seedlings transferred to the light, $^1O_2$ production appeared to be cytotoxic and led to nonenzymatic LPO and cell death (Kim et al., 2008; Przybyla et al., 2008). We observed in our experiments that the first photooxidative leave damage symptoms, which appeared in the light 4 h after the dark/light shift, were accompanied by a nonenzymatic LPO caused almost exclusively by $^1O_2$ (about 15% of the 13-LOX LPO; Supplemental Fig. S2), suggesting that $^1O_2$ cytotoxic effects may occur in photosynthetic tissues. Because we observed high levels of $^1O_2$-mediated LPO in the *vte1 npq1* mutant that directly preceded or occurred concurrently with cell death we hypothesized that $^1O_2$ produced by the photosystems is also cytotoxic, damaging the photosynthetic tissues. To validate this hypothesis, we assessed LPO events in *ch1* mutant plants that are deficient in chlorophyll *b* and PSII chlorophyll-protein antenna complexes and are characterized by a low nonphotochemical quenching (NPQ) capacity (Havaux et al., 2007). Because NPQ deactivates excited chlorophylls, thereby avoiding $^1O_2$ production, its inhibition in *ch1* leads to a highly sensitive photooxidation phenotype. Transfer of *ch1* plants pregrown at low light (20°C, 100 μmol m^{-2} s^{-1}) to photooxidative stress conditions (7°C, 1,300 μmol m^{-2} s^{-1}) at high CO_2 levels induced leaf damage within 8 h (Fig. 3A). Tissue damage was preceded by an increase of LPO after 6 h, as visualized by autoluminescence imaging (Havaux et al., 2006; Fig. 3A) and quantified by HOTE levels (Fig. 3B). Again, the HOTE signature had a typical $^1O_2$-mediated LPO signature (Fig. 3B). Both in *vte1 npq1* and *ch1* plants, cell death symptoms were observed when LPO level exceeded a threshold level of 40 to 50 nmol HOTE g^{-1} FW.

The above results indicated that $^1O_2$-mediated LPO directly precedes the onset of cell death. A similar sequence of events was seen at high and low (70 ppm) CO_2 levels, suggesting that the observed LPO and cell death were independent of photorespiratory H_2O_2. The absence of FR-mediated LPO under these conditions was confirmed by monitoring the levels of F_1-phytoprostanes (PPF_1) that are sensitive and specific markers for FR-mediated LPO (Imbusch and Mueller, 2000; Mueller, 2004). PPF_1 levels in wild-type and *ch1* leaves were below 2 nmol/g FW under low or high light conditions both at low and high CO_2 concentrations (Fig. 3C). Additional evidence of a close correlation between $^1O_2$ accumulation and cell death in *ch1* was obtained by monitoring H_2O_2 and $^1O_2$-specific marker genes (Gadjev et al., 2006; Laloi et al., 2007). We analyzed the relative expression levels of two H_2O_2-responsive genes and two $^1O_2$-responsive genes

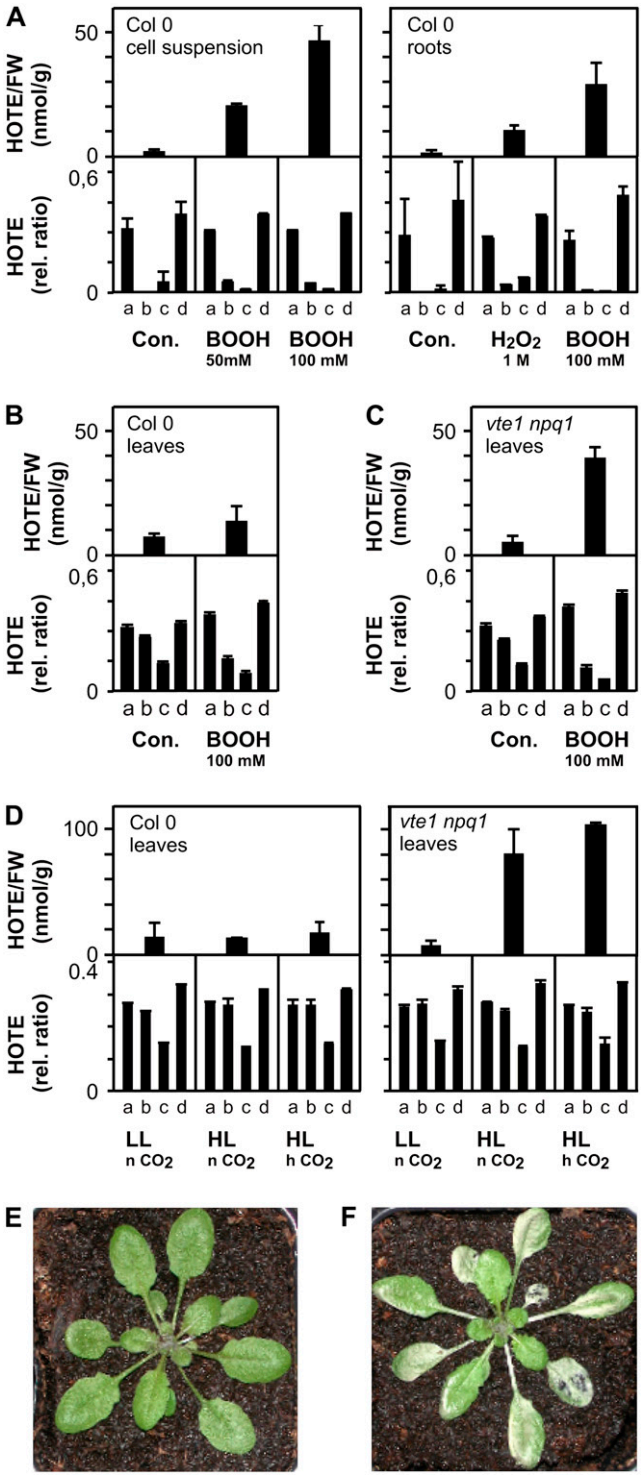

Figure 2. FR- and $^1O_2$-mediated peroxidation of 18:3 in Arabidopsis. A, ROS-mediated LPO, expressed as HOTE levels, and HOTE signature (for details, see Fig. 1) of wild-type (Col-0) cell suspensions and roots under control conditions (Con.) and after treatment with *tert*-BOOH or H_2O_2 for 4 h. B to D, ROS-mediated LPO and HOTE signature (for details, see Fig. 1) in wild-type (Col-0) and *vte1 npq1* leaves of plants grown under low light (LL = 100 μmol m^{-2} s^{-1}). B and C, Plants were kept in the dark and infiltrated with a mixture of 100 mM BOOH/5 mM Fe^{2+} for 4 h. D, Plants were stressed at 7°C, high light (HL = 1,300 μmol m^{-2} s^{-1}), and different CO_2 (n CO_2 = 380 ppm, h CO_2 = 2,000 ppm) conditions for 26 h. Results are expressed as mean ± SD ($n = 3$). E and F, Images of wild-type (E) and *vte1 npq1* (F) plants stressed with high light (1,300 μmol m^{-2} s^{-1}; 7°C) for 26 h at 2,000 ppm CO_2 showing leaf damage to the *vte1 npq1* plant.

(Fig. 3D). In high light-stressed *ch1* plants, H_2O_2 marker gene expression is maintained or slightly induced at both low and high CO_2. In agreement with the HOTE signature, $^1O_2$-specific transcripts were induced. Hence, PPF_1 and gene expression analysis confirmed that *ch1* cell death was not associated with H_2O_2 and FR-mediated LPO.

Taken together, these results indicate that the *ch1* mutant is an appropriate model system to study $^1O_2$-specific oxidative stress. Using the *vte1 npq1*, *flu*, and *ch1* genetic models, we show that $^1O_2$-mediated LPO directly precedes and/or correlates with cell death and that plastid $^1O_2$ accumulation not only is able to trigger a genetic death program, as demonstrated with the *flu* mutant (op den Camp et al., 2003; Wagner et al., 2004; Przybyla et al., 2008), but is also directly cytoxic to photosynthetic cells by oxidizing cellular components, such as lipids.

Overproduction of $O_2^{-\cdot}$ or H_2O_2 Triggers Photooxidative $^1O_2$ Formation, LPO, and Cell Death

To assess LPO signatures in plant cell death events, we monitored the LPO signature triggered by increased $O_2^{-\cdot}/H_2O_2$ levels at the PSI site by applying 1 μM methyl viologen (MV) to Arabidopsis leaf discs from plants grown either under a low or moderate light regime (100 or 250 μmol m^{-2} s^{-1}). MV is an herbicide that mimics the Mehler reaction by collecting electrons from the reduced ferredoxins at PSI and transferring them to O_2 to produce $O_2^{-\cdot}$ that is rapidly converted into H_2O_2 (Asada, 2006). Leaf discs from low light-grown plants were more sensitive than those from plants grown at moderate light, as first bleaching appeared within 26 and 50 h, respectively (data not shown). In addition, MV-induced HOTE levels were significantly higher in leaf discs from low light-grown plants (Fig. 4). Surprisingly, in both cases a strong $^1O_2$-mediated LPO was detected (Fig. 4). The mechanism of $^1O_2$ formation is not clear but is likely the result of $O_2^{-\cdot}/H_2O_2$-propagated oxidative damage of PSII and/or release of chlorophyll from damaged PS.

To determine the LPO signature provoked by increased photorespiratory H_2O_2 production, we used Cat(−) Arabidopsis plants (Vandenabeele et al., 2004) in which the activity of the major peroxisomal H_2O_2 scavenger is reduced below 10%. Cat(−) plants were grown under nonphotorespiratory conditions (low light, 100 μmol m^{-2} s^{-1}; 2,000 ppm CO_2) before transfer to photorespiration-stimulating conditions by applying 70 ppm (low level, near the compensation point), 380 ppm (normal level), or 2,000 ppm (high level) CO_2 combined with high light (700 μmol m^{-2} s^{-1}). In contrast to wild type, Cat(−) plants developed photorespiratory H_2O_2-dependent cell death within 26 h at

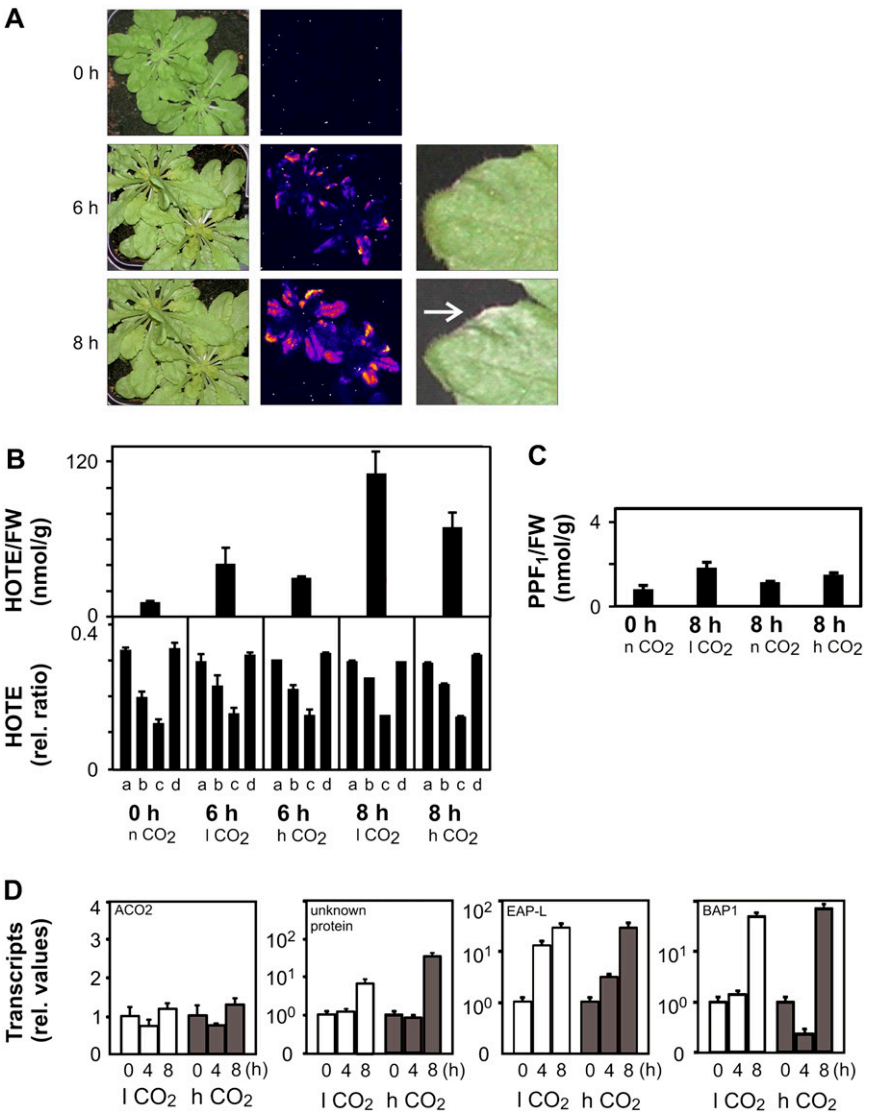

Figure 3. Photooxidation of the *ch1* Arabidopsis mutant. *ch1* plants, grown at low light (100 μmol m^{-2} s^{-1}; 20°C) under normal CO_2 (n CO_2 = 380 ppm) conditions, were stressed with high light (1,300 μmol m^{-2} s^{-1}; 7°C) at different CO_2 levels (l CO_2 = 70 ppm; n CO_2; h CO_2 = 2,000 ppm) for the time indicated. A, Images of control and stressed plants at high CO_2 after 0, 6, and 8 h; left sections, photography of the plants; middle sections, autoluminescence measurement (Havaux et al., 2006) reflecting LPO; right sections, example of damage development on a leaf. B, ROS-mediated LPO, expressed as total HOTE levels (top), and HOTE signature (bottom; for details, see Fig. 1) of leaves from *ch1* plants stressed for 0, 6, and 8 h. The HOTE signatures indicate the occurrence of $^1O_2$-mediated LPO under all conditions. C, PPF_1 levels of *ch1* plants. D, Expression of H_2O_2 (*ACO2* and unknown protein) and $^1O_2$ (EAP-like and *BAP1*) marker genes in *ch1* plants (for details, see "Materials and Methods") for the time (h) indicated. Results are expressed as mean ± SD (n = 3) for B and C, and mean ± SE (n = 6) for D.

low CO_2 (Fig. 5A) and within 50 h at normal CO_2 (data not shown). Cell death was completely inhibited at high CO_2 (Fig. 5A). H_2O_2 accumulation was reflected by an increase in phytoprostane levels and H_2O_2-responsive gene expression (Fig. 5, B and C). LPO gradually increased in Cat(−) plants, but not in wild-type plants (Fig. 6A). Like for the *ch1* mutant, tissue damage was correlated with LPO levels higher than 40 to 50 nmol HOTE g^{-1} FW. Strikingly, the HOTE isomer distribution again showed a strict $^1O_2$-mediated LPO signature (Fig. 6B), suggesting that, also in Cat(−) plants, FR-mediated LPO is a minor process. The accumulation of $^1O_2$ production was also reflected by the up-regulation of $^1O_2$ specific transcripts. As expected, transcript levels of the H_2O_2-specific marker genes had also increased (Fig. 5B). In contrast, in Cat(−) plants transferred to high light and kept at high CO_2, H_2O_2 as well as $^1O_2$ marker gene expression was maintained or only slightly and transiently induced (Fig. 5B), and $^1O_2$-mediated LPO increase (data not shown) and cell death (Fig. 5A) were completely suppressed. Hence, peroxisomal H_2O_2 overproduction ultimately leads to plastidic $^1O_2$ formation and $^1O_2$-dependent LPO preceding cell death. Taken together, our results demonstrate that, regardless of the chemical identity or subcellular production site of the initially produced ROS, plant cell death is correlated with $^1O_2$-mediated LPO.

DISCUSSION

In photosynthetic tissues, photooxidative stress involves the action of several ROS that are generated in different subcellular compartments. We established a novel method that allows us to discriminate between FR- and $^1O_2$-mediated LPO by using 10-HOTE and 15-HOTE as specific reporters of $^1O_2$-dependent LPO. Our results show that, whereas in Arabidopsis roots or cell suspensions nonenzymatic LPO depends on FRs, in leaves it is almost exclusively mediated by $^1O_2$. Notably, levels of oxidized lipids were typically an order of magnitude higher in leaf tissues than in roots. Photooxidative stress conditions in the $^1O_2$-sensitive

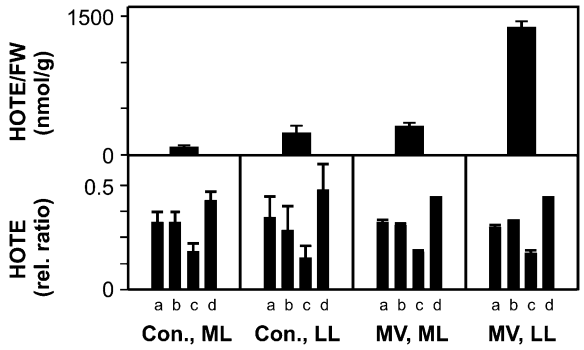

Figure 4. Photooxidation of wild-type Arabidopsis leaves treated with MV. ROS-mediated LPO, expressed as HOTE levels and HOTE signature (for details, see Fig. 1) of leaf discs from control plants (Con.) and MV-treated plants. Leaf discs of plants grown in low light (LL = 100 μmol m^{-2} s^{-1}) and moderate light (ML = 250 μmol m^{-2} s^{-1}) were incubated with or without MV (1 μM) for 30 and 50 h, respectively. The HOTE signature (for details, see Fig. 1) indicates an almost exclusive $^1O_2$ LPO mechanism under all conditions. Results are expressed as mean ± SD ($n = 3$).

vte1 npq1 double-mutant leaves provoked strongly increased $^1O_2$-mediated LPO in combination with extensive tissue damage. In addition, using the chlorophyll *b*-deficient mutant *ch1*, it was shown that accelerating the accumulation of $^1O_2$ was associated with more rapidly occurring tissue damage. Surprisingly, massive $^1O_2$-mediated LPO was also detected in leaves under conditions that favored the accumulation of $O_2^{-\cdot}$ and H_2O_2, resulting in the production of $^{\cdot}OH$ through the Fenton or Haber-Weiss reactions (Halliwell and Gutteridge, 2007). Together, these data indicate that photooxidative stress in leaf tissue results in $^1O_2$-mediated LPO, whatever the initial ROS production is, and suggest that $^1O_2$ can be directly toxic to cells.

The chemical reactivity of $^{\cdot}OH$ and $^1O_2$ toward a variety of organic scavenger molecules is almost equal and, in both cases, the reaction rate is diffusion limited (Elstner, 1982; Foyer and Noctor, 2005). The half-life of $^{\cdot}OH$ in living cells is estimated to be around 1 ns (Cheng et al., 2002). In contrast, the decay time of $^1O_2$ in cells is about 4 orders of magnitude higher (Baier et al., 2005). The decay time and the calculated diffusion path length of both species are also dependent on the microenvironment. For instance, the lifetime of $^1O_2$ in water is 3 μs and in membranes about 14 μs, corresponding to a calculated diffusion length of about 200 and 400 nm, respectively (Baier et al., 2005). To explain these differences, it is known that $^{\cdot}OH$ is the oxidizing species with the highest redox potential level (Halliwell and Gutteridge, 2007), leading to an indiscriminate hydrogen abstraction from any organic compound, whereas $^1O_2$ is acting more specifically with unsaturated compounds, according to pericyclic addition reactions. Thus, $^1O_2$ must diffuse until it reaches a suitable quencher. In algae at very high light, when the plastid $^1O_2$-scavenging capacities are overwhelmed, long-range $^1O_2$ diffusion has been experimentally measured, with $^1O_2$ being detectable outside of chloroplasts (Fischer et al., 2007). In addition to this, $^{\cdot}OH$ initiates a self-propagating radical chain reaction while $^1O_2$ reacts with a 1:1 stoichiome-

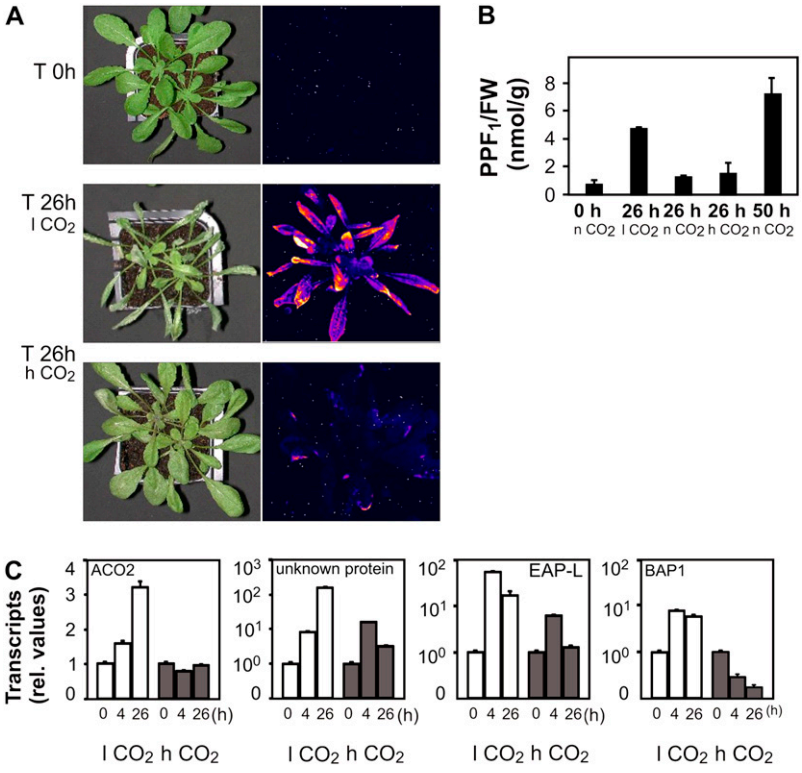

Figure 5. Photooxidation in Cat(−) Arabidopsis plants. Wild-type and Cat(−) plants were grown at low light (100 μmol m^{-2} s^{-1}) and high CO_2 levels (2,000 ppm). Stress experiments were conducted at 21°C, medium light conditions (700 μmol m^{-2} s^{-1}), and at different CO_2 levels (l CO_2 = 70 ppm; n CO_2 = 380 ppm; h CO_2 = 2,000 ppm) to modulate photorespiratory H_2O_2 production. A, Images of Cat(−) plants transferred to high light under l CO_2 and h CO_2 for 26 h. Leaf damage is observed only under l CO_2 photorespiratory conditions (left) and is accompanied by increased autoluminescence (right; Havaux et al., 2006), reflecting LPO. B, PPF_1 accumulation in Cat(−) plants under photorespiratory conditions for the time indicated. C, Expression of H_2O_2 (*ACO2* and unknown protein) and $^1O_2$ (EAP-like and *BAP1*) marker genes in Cat(−) plants (see "Materials and Methods" for details), under l CO_2 and h CO_2 stress conditions, for the time (h) indicated. Results are expressed as mean ± SD ($n = 3$) for B and as mean ± SE ($n = 6$) for C.

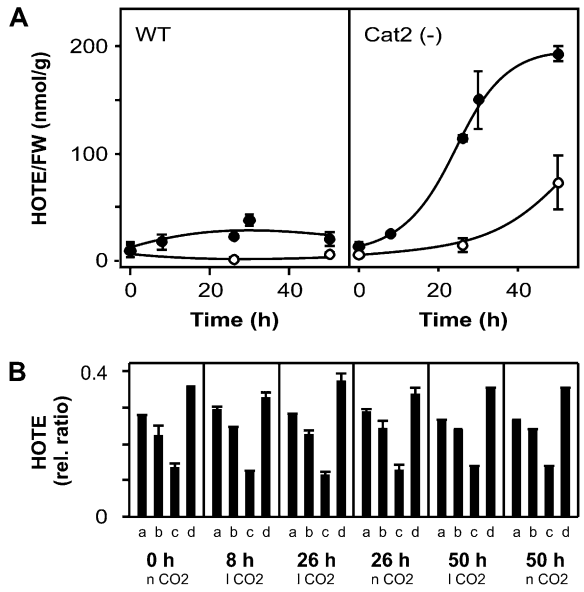

Figure 6. LPO in Cat(−) Arabidopsis plants. A, Changes in ROS-mediated LPO, expressed as HOTE levels, for wild-type and Cat(−) plants under photorespiratory stress conditions at 70 (●) or 380 ppm CO_2 (○); see Figure 5 for conditions for B. The HOTE signatures in Cat(−) plants indicate the occurrence of $^1O_2$-mediated LPO under all conditions (see Fig. 1 for details). Results are expressed as mean ± SD ($n = 3$).

try. All these considerations suggest that the relative damaging effect of equimolar concentrations of both ROS is largely in favor of $^{\cdot}OH$, therefore excluding that the $^1O_2$ signature systematically found in our leaf experiments is due to a differential reactivity of $^1O_2$ and FRs. It is established that $^{\cdot}OH$ triggers a FR-catalyzed LPO chain reaction to form phytoprostanes that are validated specific markers of FR-dependent LPO (Mueller, 2004; Thoma et al., 2004). Although we did observe that in Cat(−) leaves increased H_2O_2 levels led to FR-mediated phytoprostane accumulation, LPO still exhibited a typical $^1O_2$ signature, suggesting that FR-mediated LPO was completely overwhelmed by $^1O_2$-mediated LPO. Therefore, our results show that the most relevant ROS, which is produced in the chlorophyll-containing lipid membranes of leaf tissue exposed to light, is $^1O_2$ both under basal and stress conditions.

$^1O_2$ oxidizes cellular components, such as nucleic bases (Ravanat et al., 2000), proteins (Davies, 2003), and membranes and this characteristic is exploited in photodynamic therapies to kill cancer cells (Girotti and Kriska, 2004), bacteria (Maisch et al., 2007), and also to conceive herbicides (Fufezan et al., 2002; Tripathy et al., 2007). We have observed that $^1O_2$-mediated LPO precedes cell death in our $^1O_2$-overproducing mutants *vte1 npq1* and *ch1*. Our data suggest that $^1O_2$ production prevails over FR production and hence $^1O_2$ appears as the most relevant ROS with respect to the execution of cell death in leaf tissues. An example of ROS-dependent plant cell death is also the hypersensitive response (Torres et al., 2006) during which light seems to be required both to initiate a cell death program, early on in the infection, as well as at later stages of cell death execution (Zeier et al., 2004; Liu et al., 2007). Interestingly, $^1O_2$ HOTE markers significantly increased in Arabidopsis leaves challenged with the avirulent strain DC3000 of *Pseudomonas syringae* (Grun et al., 2007). In tobacco (*Nicotiana tabacum*), a pathogen-induced mitogen-activated protein kinase cascade disrupts chloroplast metabolism and leads to a rapid shutdown of CO_2 fixation, a phenomenon that is expected to favor light-dependent excess excitation energy conditions in thylakoids and ROS production (Liu et al., 2007). It is also worth mentioning that compromised linear electron transport in transgenic tobacco plants with reduced ferredoxin-NADP(H) reductase levels also led to increased generation of $^1O_2$, eventually followed by cell death (Palatnik et al., 2003). Apparently, environmental stresses that initiate cell death programs converge at halted chloroplast metabolism. As a result, excess light energy induces massive $^1O_2$ formation, LPO, and membrane damage that may efficiently accelerate cell death. In the dark, the actual appearance of cell death is often delayed or even abolished. Taken together, these observations suggest that, to some extent, the photoproduction of $^1O_2$ is responsible for light-dependent plant cell death. Therefore, we speculate that in chlorophyll-containing tissues, whatever the conditions of cell death initiation are, a photodynamic production of $^1O_2$ is involved in the cell death process.

Besides a putative role as a physiologically relevant cytotoxin, a signaling role for $^1O_2$ has been reported. Low subtoxic levels of $^1O_2$ that do not cause any significant LPO are apparently sufficient to trigger signaling events in bacteria (Agnez-Lima et al., 2001), cyanobacteria (Anthony et al., 2005), algae (Ledford et al., 2007), and mammalian cells (Klotz et al., 2003). In the Arabidopsis *flu* mutant, $^1O_2$ is produced by protochlorophyllides that accumulate after a dark-to-light shift hereby leading to cytotoxic effects in etiolated seedlings and to $^1O_2$-mediated stress signaling and programmed cell death in green plantlets (op den Camp et al., 2003; Wagner et al., 2004; Kim et al., 2008; Przybyla et al., 2008). In agreement with the $^1O_2$ signaling function, we observed an early accumulation of $^1O_2$-specific transcripts in light-stressed *ch1* and Cat(−) plants. We also observed that $^1O_2$-mediated LPO was always associated with enhanced autoluminescence signals and preceded cell death in our $^1O_2$-overproducing mutants. Hence, $^1O_2$ appears to be involved in two clearly separable processes, signaling and execution, with respect to cell death. Such a dual role has been previously proposed for H_2O_2 also (Apel and Hirt, 2004; Asada, 2006; Torres et al., 2006; Van Breusegem and Dat, 2006).

In summary, we show that in addition to its involvement in stress and programmed cell death-related signaling events, $^1O_2$ may be an important determinant during the execution phase of plant cell death.

MATERIALS AND METHODS

Plant Materials, Growth, and Stress Conditions

Arabidopsis (*Arabidopsis thaliana*) Heyhn. lines were issued from the Columbia ecotype (Col-0). The *vte1 npq1*, *ch1*, and Cat(−) plants have been previously described (Vandenabeele et al., 2004; Havaux et al., 2005, 2007). They were cultivated on soil under low light (100 μmol m^{-2} s^{-1}; day/night 8/16; 20°C/18°C; 70% relative humidity) and normal (380 ppm) or high CO_2 (2,000 ppm) for 4 to 5 weeks. For photooxidative stress conditions, plants were transferred in controlled chambers at the beginning of the day period (day/night 14/10), either at low temperature (7°C) and high light (1,300 μmol m^{-2} s^{-1}) or normal temperature (20°C) and medium light (700 μmol m^{-2} s^{-1}), and under various CO_2 conditions (70, 380, and 2,000 ppm). For root treatments, plants were grown on sand and then transferred in an hydroponic oxygenated device for 3 d before application of H_2O_2 or BOOH for 4 h. Arabidopsis cells of Col-0 (100 mL of cell suspension in a 250 mL Erlenmeyer flask; rotatory shaking at 125 rpm) were grown at 25°C under continuous low light (90 μmol m^{-2} s^{-1}) in Chandler's medium (Chandler et al., 1972). Cells were collected at 24% packed cell volume (15 g/100 mL) and treated similarly in the dark. For hydroperoxide application to the leaves, the treatment was carried out by infiltration of a solution of BOOH (100 mM) and $FeCl_2$ (5 mM) at the end of the night period, and 4 h incubation in the dark. For MV treatment, leaf discs (diameter 1.2 cm) of Col-0 plants were floated for 30 to 50 h on a Tween 20 (0.1%) solution with or without 1 μM MV.

PUFA Oxidation

PUFAs (3–5 mg of 18:2 or 18:3) as a slurry mixture in methanol/water (0.5/1.5 mL) were oxidized (1) by 0.1 mM methylene blue in the light (300–340 μmol m^{-2} s^{-1}) to generate $^1O_2$; or (2) by 50 mM H_2O_2 or BOOH (5–10 mM) in the presence of 0.5 mM $FeCl_2$ to generate FRs. The reaction was incubated for 10 to 120 min and stopped by adding 1 mL of $CHCl_3$ containing 1 mg/mL triphenyl phosphine and 0.05% (w/v) butylated hydroxytoluene. The organic phase was recovered and analyzed for hydroxy fatty acid content and distribution.

LPO Analyses

Imaged autoluminescence signal is attributed to the spontaneous decomposition of peroxides (Havaux et al., 2006). Spontaneous photon emission from whole Arabidopsis plants was measured after 2 h dark adaptation with a liquid N_2 cooled CCD camera, as previously described (Havaux et al., 2005, 2007). Integration time was 20 min. For hydroxy fatty acid analyses, lipids were extracted from 0.5 g frozen plant material by grinding with 2 × 1 mL $CHCl_3$ containing 1 mg/mL triphenyl phosphine and 0.05% (w/v) butylated hydroxytoluene, with 15-hydroxy-11,13(*Z*,*E*)-eicosadienoic acid as internal standard. The organic phase was evaporated under a stream of N_2. The residue was recovered in 1.25 mL ethanol and 1.25 mL 3.5 M NaOH and hydrolyzed at 80°C for 15 min. After addition of 2.2 mL 1 M citric acid, hydroxy fatty acids were extracted with 2 × 1 mL hexane/ether (50/50). The organic phase was used for the straight phase HPLC-UV analysis, as previously described (Montillet et al., 2004). PPF_1 extraction was carried out on 0.5 g frozen material, as previously described (Imbusch and Mueller, 2000). For the HPLC-electrospray ionization-MS/MS analyses, aliquots were evaporated and recovered in aqueous 1 mM ammonium acetate/acetonitrile (60:40, v/v) with [$^{18}O_2$]13-HOTE or [$^{18}O_3$]PPF_1 used as internal standards. Hydroxy fatty acids were separated by HPLC on a Purospher Star RP-18e column (125 × 2 mm i.d., 5 μm particle size, Merck). HOTE were eluted from the column using a linear gradient (0.2 mL/min) starting with 1 mM ammonium acetate in water/acetonitrile (65:35, v/v) at 0 min to 40:60 (v/v) at 10 min. PPF_1 were eluted with a linear gradient starting with 90:10 (v/v) at 0 min to 60:40 (v/v) at 15 min. Hydroxy fatty acids and PPF_1 were analyzed using a Waters Micromass Quatro Premier triple quatrupole mass spectrometer in the negative electrospray ionization mode (for conditions, see Supplemental Table S1).

RNA Isolation and Quantitative Reverse Transcription-PCR

For each sample, RNA was isolated from leaves of four plants with the TRIzol reagent (Invitrogen). First-strand cDNA was prepared using 2.5 μg total RNA, Superscript II reverse transcriptase (Invitrogen), and an oligo(dT)15 primer. Five microliters of 1:6 or 1:12 diluted first-strand cDNA was used as a template in the subsequent PCR, performed on a Bio-Rad iCycler using 200 nM primers and Platinum Supermix-UDG (Invitrogen) supplemented with fluorescein dye in a final volume of 25 μL per reaction, according to the manufacturer's instructions. All PCR reactions were performed in triplicate on material from two biological repeat experiments. The H_2O_2-specific genes used were At1g49150 (unknown protein) and At1g62380 (*ACO2*), the $^1O_2$-specific genes At5g10830 (embryo abundant protein-like) and At3g61190 (*BAP1*; Gadjev et al., 2006; Laloi et al., 2007). Universal ProbeLibrary probes (Roche Applied Science) and primers used can be found in Supplemental Table S2. All transcript levels were normalized using actin-related protein 7 (At3g60830) as a control gene.

Supplemental Data

The following materials are available in the online version of this article.

Supplemental Figure S1. Hydroxy fatty acid distribution for the oxidation of linoleic (18:2) and linolenic (18:3) acids.

Supplemental Figure S2. Photooxidation of the *flu* Arabidopsis mutant.

Supplemental Table S1. Mass transitions and conditions for negative electrospray ionization HPLC-MS/MS analysis of PPF_1 and of the hydroxy fatty acids issued from the oxidation of linoleic (18:2) and linolenic (18:3) acids.

Supplemental Table S2. Primers and universal probe library probes (Roche Applied Science) that were used in the quantitative PCR reactions.

ACKNOWLEDGMENTS

We thank Christophe Laloi (ETH, Zurich) for helpful discussions; Jean-Luc Montillet (IBEB, CEA Cadarache) for the root and cell experiments; Michaël Vandorpe (DPSB, Ghent) for excellent technical assistance; Martine De Cock (DPSB, Ghent) for help in preparing the manuscript; and the Groupe de Recherche Appliquée en Phytotechnie (CEA Cadarache) for the controlled growth facilities.

Received July 4, 2008; accepted July 27, 2008; published August 1, 2008.

LITERATURE CITED

Agnez-Lima LF, Di Mascio P, Demple B, Menck CFM (2001) Singlet molecular oxygen triggers the *soxRS* regulon of *Escherichia coli*. Biol Chem **382:** 1071–1075

Anthony JR, Warczak KL, Donohue TJ (2005) A transcriptional response to singlet oxygen, a toxic byproduct of photosynthesis. Proc Natl Acad Sci USA **102:** 6502–6507

Apel K, Hirt H (2004) Reactive oxygen species: metabolism, oxidative stress, and signal transduction. Annu Rev Plant Biol **55:** 373–399

Asada K (2006) Production and scavenging of reactive oxygen species in chloroplasts and their functions. Plant Physiol **141:** 391–396

Baier J, Maier M, Engl R, Landthaler M, Baumler W (2005) Time-resolved investigations of singlet oxygen luminescence in water, in phosphatidylcholine, and in aqueous suspensions of phosphatidylcholine or HT29 cells. J Phys Chem B **109:** 3041–3046

Chandler MT, Tandeau de Marsac N, Kouchkovsky Y (1972) Photosynthetic growth of tobacco cells in liquid suspension. Can J Bot **50:** 2265–2270

Cheng FC, Jen JF, Tsai TH (2002) Hydroxyl radical in living systems and its separation methods. J Chromatogr B Analyt Technol Biomed Life Sci **781:** 481–496

Dat JF, Pellinen R, Beeckman T, Van De Cotte B, Langebartels C, Kangasjärvi J, Inzé D, Van Breusegem F (2003) Changes in hydrogen peroxide homeostasis trigger an active cell death process in tobacco. Plant J **33:** 621–632

Davies MJ (2003) Reactive species formed on proteins exposed to singlet oxygen. Photochem Photobiol Sci **3:** 17–25

Elstner EF (1982) Oxygen activation and oxygen toxicity. Annu Rev Plant Physiol **33:** 73–96

Fischer BB, Krieger-Liszkay A, Hideg E, Snyrychová I, Wiesendanger M, Eggen RI (2007) Role of singlet oxygen in chloroplast to nucleus retrograde signaling in *Chlamydomonas reinhardtii*. FEBS Lett **581:** 5555–5560

Foyer CH, Noctor G (2005) Redox homeostasis and antioxidant signaling: a metabolic interface between stress perception and physiological responses. Plant Cell **17:** 1866–1875

Fufezan C, Rutherford AW, Krieger-Liszkay A (2002) Singlet oxygen production in herbicide-treated photosystem II. FEBS Lett **532:** 407–410

Gadjev I, Vanderauwera S, Gechev TS, Laloi C, Minkov IN, Shulaev V, Apel K, Inzé D, Mittler R, Van Breusegem F (2006) Transcriptomic footprints disclose specificity of reactive oxygen species signaling in Arabidopsis. Plant Physiol **141:** 436–445

Girotti AW, Kriska T (2004) Role of lipid hydroperoxides in photo-oxidative stress signaling. Antioxid Redox Signal **6:** 301–310

Grun C, Berger S, Matthes D, Mueller MJ (2007) Early accumulation of non-enzymatically synthesised oxylipins in *Arabidopsis thaliana* after infection with *Pseudomonas syringae*. Funct Plant Biol **34:** 65–71

Halliwell B, Gutteridge J (2007) Free Radicals in Biology and Medicine, Ed 4. Oxford University Press, Oxford

Havaux M, Dall'Osto L, Bassi R (2007) Zeaxanthin has enhanced antioxidant capacity with respect to all other xanthophylls in Arabidopsis leaves and functions independent of binding to PSII antennae. Plant Physiol **145:** 1506–1520

Havaux M, Eymery F, Porfirova S, Rey P, Dörmann P (2005) Vitamin E protects against photoinhibition and photooxidative stress in *Arabidopsis thaliana*. Plant Cell **17:** 3451–3469

Havaux M, Triantaphylidès C, Genty B (2006) Autoluminescence imaging: a non-invasive tool for mapping oxidative stress. Trends Plant Sci **11:** 480–484

Imbusch R, Mueller MJ (2000) Analysis of oxidative stress and wound-inducible dinor isoprostanes F_1 (phytoprostanes F_1) in plants. Plant Physiol **124:** 1293–1304

Kim C, Meskauskiene R, Apel K, Laloi C (2008) No single way to understand singlet oxygen signalling in plants. EMBO Rep **9:** 435–439

Klotz LO, Kröncke KD, Sies H (2003) Singlet oxygen-induced signaling effects in mammalian cells. Photochem Photobiol Sci **2:** 88–94

Krieger-Liszkay A (2005) Singlet oxygen production in photosynthesis. J Exp Bot **56:** 337–346

Laloi C, Stachowiak M, Pers-Kamczyc E, Warzych E, Murgia I, Apel K (2007) Cross-talk between singlet oxygen- and hydrogen peroxide-dependent signaling of stress responses in *Arabidopsis thaliana*. Proc Natl Acad Sci USA **104:** 672–677

Ledford HK, Chin BL, Niyogi KK (2007) Acclimation to singlet oxygen stress in *Chlamydomonas reinhardtii*. Eukaryot Cell **6:** 919–930

Liu Y, Ren D, Pike S, Pallardy S, Gassmann W, Zhang S (2007) Chloroplast-generated reactive oxygen species are involved in hypersensitive response-like cell death mediated by a mitogen-activated protein kinase cascade. Plant J **51:** 941–954

Maisch T, Baier J, Franz B, Maier M, Landthaler M, Szeimies RM, Bäumler W (2007) The role of singlet oxygen and oxygen concentration in photodynamic inactivation of bacteria. Proc Natl Acad Sci USA **104:** 7223–7228

Mittler R, Vanderauwera S, Gollery M, Van Breusegem F (2004) The reactive oxygen gene network in plants. Trends Plant Sci **9:** 490–498

Montillet JL, Cacas JL, Garnier L, Montané MH, Douki T, Bessoule JJ, Polkowska-Kowalczyk L, Maciejewska U, Agnel JP, Vial A, et al (2004) The upstream oxylipin profile of *Arabidopsis thaliana*: a tool to scan for oxidative stresses. Plant J **40:** 439–451

Mueller MJ (2004) Archetype signals in plants: the phytoprostanes. Curr Opin Plant Biol **7:** 441–448

Mueller MJ, Mène-Saffrané L, Grun C, Karg K, Farmer EE (2006) Oxylipins analysis methods. Plant J **45:** 472–489

op den Camp RGL, Przybyla D, Ochsenbein C, Laloi C, Kim C, Danon A, Wagner D, Hideg E, Göbel C, Feussner I, et al (2003) Rapid induction of distinct stress responses after the release of singlet oxygen in *Arabidopsis*. Plant Cell **15:** 2320–2332

Palatnik JF, Tognetti VB, Poli HO, Rodríguez RE, Blanco N, Gattuso M, Hajirezaei M-R, Sonnewald U, Valle EM, Carrillo N (2003) Transgenic tobacco plants expressing antisense ferredoxin-NADP(H) reductase transcripts display increased susceptibility to photo-oxidative damage. Plant J **35:** 332–341

Pnueli L, Liang H, Rozenberg M, Mittler R (2003) Growth suppression, altered stomatal responses, and augmented induction of heat shock proteins in cytosolic ascorbate peroxidase (*Apx1*)-deficient *Arabidopsis* plants. Plant J **34:** 187–203

Przybyla D, Göbel C, Imboden A, Hamberg M, Feussner I, Apel K (2008) Enzymatic, but not non-enzymatic $^1O_2$-mediated peroxidation of polyunsaturated fatty acids forms part of the EXECUTER1-dependent stress response program in the *flu* mutant of *Arabidopsis thaliana*. Plant J **54:** 236–248

Queval G, Issakidis-Bourguet E, Hoeberichts FA, Vandorpe M, Gakière B, Vanacker H, Miginiac-Maslow M, Van Breusegem F, Noctor G (2007) Conditional oxidative stress responses in the Arabidopsis photorespiratory mutant *cat2* demonstrate that redox state is a key modulator of daylength-dependent gene expression, and define photoperiod as a crucial factor in the regulation of H_2O_2-induced cell death. Plant J **52:** 640–657

Ravanat JL, Di Mascio P, Martinez GR, Medeiros MHG, Cadet J (2000) Singlet oxygen induces oxidation of cellular DNA. J Biol Chem **275:** 40601–40604

Rizhsky L, Liang H, Mittler R (2003) The water-water cycle is essential for chloroplast protection in the absence of stress. J Biol Chem **278:** 38921–38925

Stratton SP, Liebler DC (1997) Determination of singlet oxygen-specific versus radical-mediated lipid peroxidation in photosensitized oxidation of lipid bilayers: effect of β-carotene and α-tocopherol. Biochemistry **36:** 12911–12920

Thoma I, Krischke M, Loeffler C, Mueller MJ (2004) The isoprostanoid pathway in plants. Chem Phys Lipids **128:** 135–148

Torres MA, Jones JDG, Dangl JL (2006) Reactive oxygen species signaling in response to pathogens. Plant Physiol **141:** 373–378

Tripathy BC, Mohapatra A, Gupta I (2007) Impairment of the photosynthetic apparatus by oxidative stress induced by photosensitization reaction of protoporphyrin IX. Biochim Biophys Acta **1767:** 860–868

Van Breusegem F, Dat JF (2006) Reactive oxygen species in plant cell death. Plant Physiol **141:** 384–390

Vandenabeele S, Vanderauwera S, Vuylsteke M, Rombauts S, Langebartels C, Seidlitz HK, Zabeau M, Van Montagu M, Inzé D, Van Breusegem F (2004) Catalase deficiency drastically affects gene expression induced by high light in *Arabidopsis thaliana*. Plant J **39:** 45–58

Wagner D, Przybyla D, op den Camp R, Kim C, Landgraf F, Lee KP, Würsch M, Laloi C, Nater M, Hideg E, et al (2004) The genetic basis of singlet oxygen-induced stress responses of *Arabidopsis thaliana*. Science **306:** 1183–1185

Zeier J, Pink B, Mueller MJ, Berger S (2004) Light conditions influence specific defence responses in incompatible plant-pathogen interactions: uncoupling systemic resistance from salicylic acid and PR-1 accumulation. Planta **219:** 673–683